

AN INVESTIGATION ON CONSTRUCTION
SEQUENCE OF IRREGULAR MULTI-LAYER PRISM
TENSEGRITY

LOW ZHAO XUAN

SCHOOL OF CIVIL ENGINEERING
UNIVERSITI SAINS MALAYSIA
2018

AN INVESTIGATION ON CONSTRUCTION SEQUENCE OF
IRREGULAR MULTI-LAYER PRISM TENSEGRITY

By

LOW ZHAO XUAN

This dissertation is submitted to

UNIVERSITI SAINS MALAYSIA

As partial fulfilment of requirement for the degree of

**BACHELOR OF ENGINEERING (HONS.)
(CIVIL ENGINEERING)**

School of Civil Engineering
Universiti Sains Malaysia

June 2018



**SCHOOL OF CIVIL ENGINEERING
ACADEMIC SESSION 2017/2018**

**FINAL YEAR PROJECT EAA492/6
DISSERTATION ENDORSEMENT FORM**

Title: AN INVESTIGATION ON CONSTRUCTION SEQUENCE
OF IRREGULAR MULTI-LAYER TENSEGRITY

Name of Student: LOW ZHAO XUAN

I hereby declare that all corrections and comments made by the supervisor(s) and
examiner have been taken into consideration and rectified accordingly.

Signature:

Approved by:

(Signature of Supervisor)

Date :

Name of Supervisor :

Date :

Approved by:

(Signature of Examiner)

Name of Examiner :

Date :

ACKNOWLEDGEMENT

I would first like to thank my supervisor, Associate Professor Ir. Dr. Choong Kok Keong of the School of Civil Engineering at Universiti Sains Malaysia. He has consistently supervised me whenever I ran into trouble or had a question about my research or writing. He has given me continuous support and knowledge that steered me into the right direction.

I would also like to thank the technicians of School of Civil Engineering at Universiti Sains Malaysia who were involved in preparing the tools and equipment I needed to conduct the tests and the construction of the physical models. Without their help, this research could not have been successfully completed.

I would also like to acknowledge the volunteers who participated in the construction of the physical models. Without their passionate participation, the construction of the physical models could not have been completed smoothly.

Finally, I must express my very profound gratitude to my parents for providing me with unfailing support and continuous encouragement throughout the process of my research and thesis writing. This accomplishment would not have been possible without them.

ABSTRAK

Struktur *tensegrity* ialah sebuah struktur di mana ahli mampatan disambungkan oleh ahli tegangan. Struktur ini menunjukkan ketegarannya melalui keseimbangan diri di antara ahli mampatan dan ahli tegangan dengan memperkenalkan pra-tekanan. Pembinaan struktur *tensegrity* amat mencabar disebabkan tahap sensitivitinya yang tinggi dan ketidakstabilan bentuknya semasa proses pembinaan. Namun, kajian tentang urutan pembinaan struktur *tensegrity* skala penuh agak kekurangan. Oleh itu, kajian aplikasi hasil penentuan bentuk dan pra-tekanan kepada pembinaan struktur *tensegrity* termasuk pertimbangan isu praktikal amat diperlukan. Tumpuan kajian ini merupakan *tensegrity* prisma pelbagai lapisan secara tidak seragam. Kaedah pengiraan komputer yang menggunakan pendekatan linear dengan menggabungkan syarat hubungan panjangnya dan persamaan keseimbangan daya telah digunakan dalam proses penentuan bentuk dan pra-tekanan. Daya pra-tekanan di dalam kabel diperkenalkan melalui pemanjangan kabel. Urutan pembinaan struktur *tensegrity* telah dikaji dan ditambah baik melalui pembinaan model fizikal. Kesan urutan pembinaan pada konfigurasi muktamad struktur *tensegrity* prisma pelbagai lapisan telah dikaji. Urutan pembinaan yang terperinci mengenai struktur *tensegrity* prisma pelbagai lapisan telah dicadangkan.

ABSTRACT

Tensegrity structures are structures where its compression members (struts) are connected by continuous tension members (cables). The structure shows its rigidity through the self-equilibrium between the struts and the cables with the introduction of pre-stress. The construction of tensegrity structures is challenging due to its high sensitivity where its shape is unstable during construction. However, studies or literature on construction sequence of full scale tensegrity structures is relatively lacking. Hence, the study on application of form-finding results to the eventual construction of a tensegrity considering practical issues is needed. The focus of this study is irregular multi-layer prism tensegrity. A computational tool which uses a linear approach by combining length relation condition and force equilibrium equation is used in the form-finding process. The pre-stressing forces in the cables are applied based on the elongation of the cables. The construction sequence is investigated and improved through the erection of physical models. The effect of the construction sequence on the final configuration of the multi-layer prism tensegrity is studied. A detailed construction sequence of multi-layer prism tensegrity is proposed.

TABLE OF CONTENTS

ACKNOWLEDGEMENT	II
ABSTRAK	III
ABSTRACT	IV
TABLE OF CONTENTS	V
LIST OF FIGURES	VII
LIST OF TABLES	XI
CHAPTER 1 INTRODUCTION	1
1.1 Background	1
1.2 Problem Statement	8
1.3 Objectives.....	9
1.4 Layout of thesis	9
CHAPTER 2 LITERATURE REVIEW	10
2.1 Form-finding of tensegrity structure	10
2.2 Construction of tensegrity structure	12
2.3 Summary	20
CHAPTER 3 METHODOLOGY	21
3.1 Overview	21
3.2 Form-finding of tensegrity	23
3.3 Selection of material.....	34
3.4 Connection	35
3.5 Tensile test.....	36
3.6 Physical modelling	38
CHAPTER 4 RESULTS AND DISCUSSION	40
4.1 Overview	40
4.2 Small laboratory scale model	40
4.3 Medium laboratory scale model.....	72
4.4 Actual practical scale model	89
4.5 Discussion	113

4.6	Summary	115
CHAPTER 5 CONCLUSIONS AND RECOMMENDATIONS		116
5.1	Conclusion.....	116
5.2	Limitation and recommendation	117
REFERENCES.....		118

LIST OF FIGURES

Figure 1.1: A simple tensegrity structure (www.tensegriteit.nl)	1
Figure 1.2: The first tensegrity structure by Kenneth Snelson in 1948 – the “X-piece”. (Snelson, 2012).....	2
Figure 1.3: An example of prism tensegrity (Bansod et al., 2014).....	3
Figure 1.4: An example of diamond tensegrity (Bansod et al., 2014).....	4
Figure 1.5: An example of zig-zag tensegrity (Bansod et al., 2014)	4
Figure 1.6: Formation of multi-layer prism tensegrity from two single-layer prism tensegrity (Mohammad, 2016)	5
Figure 1.7: Example of multi-layer prism tensegrity (a) double layer tensegrity structure, (b) triple layer tensegrity structure, (c) six-layer tensegrity structure forming into an arch structure (Mohammad, 2016)	6
Figure 1.8: Examples of irregular prism tensegrity (a) single-layer tensegrity, (b) multi-layer tensegrity (www.tensegriteit.nl)	7
Figure 1.9: Interior view of White Rhino (Kawaguchi and Shunji, 2009)	7
Figure 2.1: Exterior view of the White Rhino (https://www.iis.u-tokyo.ac.jp).....	13
Figure 2.2: Plan and section view of the White Rhino (Kawaguchi and Shunji, 2009)	13
Figure 2.3: Video clippings showing the construction process of the White Rhino (https://www.youtube.com/watch?v=IeWWPAckC5U)	14
Figure 2.4: Interior view of the La Plata Stadium (http://www.stadiumguide.com/ciudaddeplata/)	15
Figure 2.5: Schematic roof frame of the La Plata Stadium (http://tensegritywiki.com/La+Plata+Stadium).....	15
Figure 2.6: Images during the construction phase of the La Plata Stadium (https://www.gettyimages.com/event/construction-of-ciudad-de-la-plata-stadium-106786978#general-view-of-the-ciudad-de-la-plata-stadium-construction-on-19-picture-id107087733)	16
Figure 2.7: The Kurilpa Bridge in Australia completed in October 2009 (https://www.arup.com/projects/kurilpa-bridge).....	17
Figure 2.8: The modelling and design of the bridge at different construction stages (http://www.oasys-software.com/solutions/case-studies.html?id=64/)	18
Figure 2.9: Laboratory scale models in triangular prism (left) and quadrilateral prism (right) with a height of 260mm (Ong, 2017).....	19
Figure 2.10: Actual practical scale model with a height of 1.8m (Ong, 2017).....	19
Figure 3.1: The flow chart of research methodology.....	23

Figure 3.2: Six joints of the first and second polygon with their connected members (Mohammad, 2016).....	25
Figure 3.3: The four subsequent joints of the connection polygon (Mohammad, 2016)	27
Figure 3.4: Interface at the input data of the first layer	30
Figure 3.5: Interface at the output data of the first layer	31
Figure 3.6: Formation of the first layer of tensegrity structure (a) first ring, (b) diagonal tension cables, (c) diagonal compression struts, (d) connection polygon.....	31
Figure 3.7: Interface at the input data of the second layer.....	32
Figure 3.8: Interface at the output data of the second layer.....	33
Figure 3.9: Formation of second layer of tensegrity structure (a) continuation from the first layer, (b) diagonal tension cables, (c) diagonal compression struts, (d) second ring.....	34
Figure 3.10: Elongation of cable when tensile force is applied.....	37
Figure 3.11: The base size of all four models.....	39
Figure 4.1: 3D visualisation of Model 1 using AUTOCAD.....	43
Figure 4.2: Connection details at a joint of Model 1	46
Figure 4.3: Placement of the compression members of the first layer.....	47
Figure 4.4: Bottom support of the compression members of the first layer	47
Figure 4.5: Cables of the first ring of the first layer is connected	48
Figure 4.6: Placement of the compression members of the second layer.....	48
Figure 4.7: Cables of the second ring of the first layer and the first ring of the second layer are connected	49
Figure 4.8: Cables of the second ring of the second layer are connected.....	49
Figure 4.9: Diagonal cables of the first layer are connected.....	50
Figure 4.10: Diagonal cables of the second layer are connected.....	50
Figure 4.11: Different views of Model 1	51
Figure 4.12: 3D visualisation of Model 2 using AUTOCAD.....	55
Figure 4.13: Placement of the compression members of the first layer.....	59
Figure 4.14: Bottom support of the compression members of the first layer	59
Figure 4.15: Cables of the first ring of the first layer is connected	60
Figure 4.16: Placement of the compression members of the second layer.....	60
Figure 4.17: Cables of the second ring of the first layer and the first ring of the second layer are connected	61

Figure 4.18: Cables of the second ring of the second layer are connected	61
Figure 4.19: Diagonal cables of the first layer are connected.....	62
Figure 4.20: Diagonal cables of the second layer are connected.....	62
Figure 4.21: Different views of Model 2	63
Figure 4.22: Differences of Model 1 compared to the results of form-finding analysis in plan view	67
Figure 4.23: Differences of Model 2 compared to results of form-finding analysis in plan view.....	70
Figure 4.24: Fishing line test using dead load	71
Figure 4.25: Tightening of knot which contributed to the extension of the overall length of the cable.....	71
Figure 4.26: 3D visualisation of Model 3 using AUTOCAD.....	75
Figure 4.27: Connection detail at a joint.....	77
Figure 4.28: Connection details of Model 3	78
Figure 4.29: The testing of the cable of Model 3.....	78
Figure 4.30: Graph of force against elongation of cable sample 1	80
Figure 4.31: Cables of the first ring of the first layer is connected	82
Figure 4.32: Cables of the second ring of the first layer and the first ring of the second layer are connected	82
Figure 4.33: Cables of the second ring of the second layer are connected	83
Figure 4.34: Diagonal cables of the first layer are connected.....	83
Figure 4.35: Diagonal cables of the second layer are connected.....	84
Figure 4.36: Different views of Model 3	85
Figure 4.37: Projecting the coordinates of joint into plan view.....	86
Figure 4.38: Measuring the height of the joint	86
Figure 4.39: Differences of Model 3 compared to the results of form-finding analysis in plan view	89
Figure 4.40: 3D visualisation of Model 4 using AUTOCAD.....	93
Figure 4.41: Connection details of Model 4	95
Figure 4.42: The testing of cable of Model 4.....	96
Figure 4.43: The cable of Model 4 at failure	96
Figure 4.44: Graph of force against elongation of cable sample 2	97
Figure 4.45: Testing of connection between cable and aluminium tube of Model 4.....	98
Figure 4.46: Testing of connection between cable and turnbuckle of Model 4.....	99

Figure 4.47: The support at the bottom part of the compression member of the first layer of Model 4	102
Figure 4.48: Cables of the first ring of the first layer is connected	102
Figure 4.49: Cables of the second ring of the first layer and the first ring of the second layer are connected	103
Figure 4.50: Cables of the second ring of the second layer are connected	103
Figure 4.51: Diagonal cables of the second layer are connected	104
Figure 4.52: Different views of Model 4	105
Figure 4.53: Projecting the coordinates of joint into plan view.....	107
Figure 4.54: Measuring the height of the midpoint of the member	107
Figure 4.55: Differences of Model 4 compared to the results of form-finding analysis in plan view	111
Figure 4.56: Verification of pre-stressing force applied in the cable	112

LIST OF TABLES

Table 4.1: Coordinates of joints of the first ring of the first layer of Model 1	41
Table 4.2: Coordinates of centroid of the second ring of the first layer of Model 1	41
Table 4.3: Coordinates of the second ring of the first layer of Model 1	41
Table 4.4: Coordinates of the second conjunction polygon of the first layer of Model 1.....	42
Table 4.5: Coordinates of the centroid of the second ring of the second layer of Model 1	42
Table 4.6: Coordinates of the second ring of the second layer of Model 1	43
Table 4.7: Force ratio and final length of each member of Model 1	44
Table 4.8: Elongation and shortened length of the cables with respect to the force applied of Model 1	45
Table 4.9: Coordinates of joints of the first ring of the first layer of Model 2	52
Table 4.10: Coordinates of centroid of the second ring of the first layer of Model 2 ...	52
Table 4.11: Coordinates of the second ring of the first layer of Model 2.....	53
Table 4.12: Coordinates of the second conjunction polygon of the first layer of Model 2.....	53
Table 4.13: Coordinates of centroid of the second ring of the second layer of Model 2	53
Table 4.14: Coordinates of the second ring of the second layer of Model 2	54
Table 4.15: Force ratio and final length of each member of Model 2	56
Table 4.16: Elongation and shortened length of the cables with respect to the force applied of Model 2	57
Table 4.17: Comparison of coordinates of joints of Model 1	65
Table 4.18: Comparison of length of members of Model 1	66
Table 4.19: Comparison of coordinates of joints of Model 2	67
Table 4.20: Comparison of length of members of Model 2.....	69
Table 4.21: Coordinates of joints of the first ring of the first layer of Model 3	72
Table 4.22: Coordinates of centroid of the second ring of the first layer of Model 3 ...	72
Table 4.23: Coordinates of the second ring of the first layer of Model 3.....	73
Table 4.24: Coordinates of the second conjunction polygon of the first layer of Model 3.....	73

Table 4.25: Coordinates of centroid of the second ring of the second layer of Model 3	73
Table 4.26: Coordinates of the second ring of the second layer of Model 3	74
Table 4.27: Force ratio and final length of each member of Model 3	76
Table 4.28: Result of tensile test of the cable of Model 3	79
Table 4.29: Result of force and elongation based on cable sample 1	80
Table 4.30: Elongation and shortened length of the cables of Model 3	81
Table 4.31: Comparison of coordinates of joints of Model 3	87
Table 4.32: Comparison of length of members of Model 3.....	88
Table 4.33: Coordinates of joints of the first ring of the first layer of Model 4	90
Table 4.34: Coordinates of centroid of the second ring of the first layer of Model 4 ...	90
Table 4.35: Coordinates of the second ring of the first layer of Model 4.....	91
Table 4.36: Coordinates of the second conjunction polygon of the first layer of Model 4.....	91
Table 4.37: Coordinates of centroid of the second ring of the second layer of Model 4	91
Table 4.38: Coordinates of the second ring of the second layer of Model 4	92
Table 4.39: Force ratio and final length of each member of Model 4	94
Table 4.40: Result of tensile test of the cable of Model 4	97
Table 4.41: Result of tensile test of the connection between cable and aluminium tube of Model 4.....	99
Table 4.42: Result of tensile test of the connection between cable and turnbuckle of Model 4.....	99
Table 4.43: Result of force and elongation based on cable sample 2	100
Table 4.44: Elongation and shortened length of the cables of Model 4	101
Table 4.45: Comparison of coordinates of midpoint of each member of Model 4.....	108
Table 4.46: Comparison of length of members of Model 4.....	110
Table 4.47: Compensation of the increased length of joint by shortening the length of the turnbuckle	112
Table 4.48: Result of verification of pre-stressing force applied in the cable	113

CHAPTER 1

INTRODUCTION

1.1 Background

Tensegrity structures are structures where its compression members (struts) are connected by continuous tension members (cables). The structure shows its rigidity through the self-equilibrium between the struts and the cables with the introduction of pre-stress. Figure 1.1 shows a simple tensegrity structure which consists of the compression members (struts) and the tension members (cables).

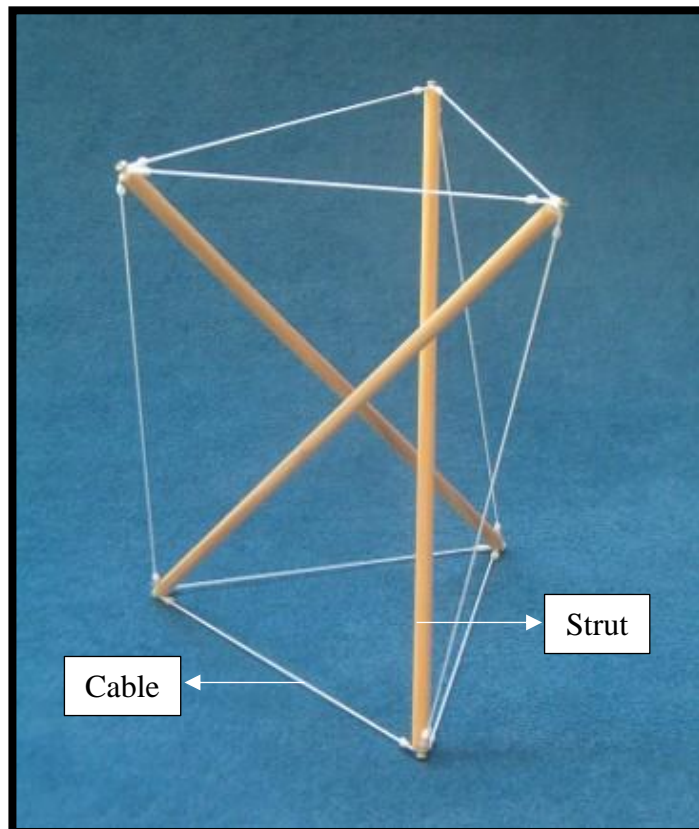


Figure 1.1: A simple tensegrity structure (www.tensegriteit.nl)

The very first tensegrity structure was built by Kenneth Snelson in 1948 (Snelson, 2012). The “X-piece” as shown in Figure 1.2 was the first tensegrity structure built by Kenneth Snelson. The term tensegrity was coined by Richard Buckminster Fuller as a contraction of “tensional integrity”. Buckminster (1962) describes that tensegrity structures will have the aspect of continuous tension throughout and the compression will be subjugated so that the compression elements become small islands in a sea of tension. The definition of tensegrity is also given by other authors. Pugh (1976) gives the definition of tensegrity as a system established when a set of discontinuous compressive components interacts with a set of continuous tensile components to define a stable volume in space. Motro (2003) further expressed the definition of tensegrity as a system in a stable self-equilibrated state comprising a discontinuous set of compressed components inside a continuum of tensioned components.

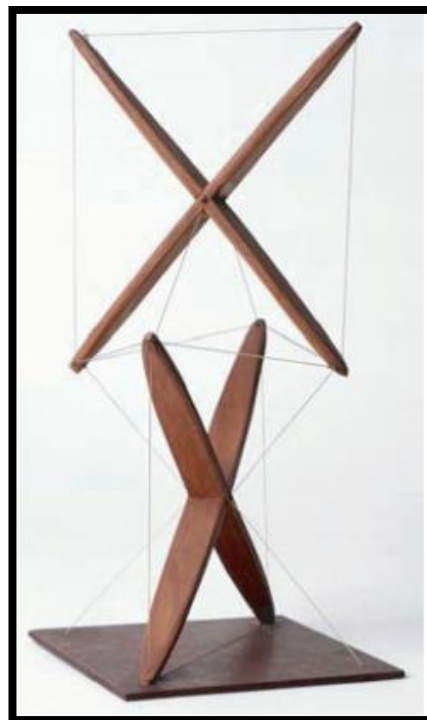


Figure 1.2: The first tensegrity structure by Kenneth Snelson in 1948 – the “X-piece”.
(Snelson, 2012)

Tensegrity structures come in various types and configurations. Bansod et al. (2014) classified tensegrity structures into three main categories which are prism tensegrity, diamond tensegrity and zig-zag tensegrity. The prism tensegrity can be considered as a twisted prism consisting of two triangular faces twisted with respect to each other. The two triangular faces can be considered as a bottom ring and a top ring which are parallel in plane with each ring indicating each level of the structure. The struts are located diagonally between the vertices of both rings. Diagonal cables are connected between the two levels of ring. Figure 1.3 shows an example of prism tensegrity.

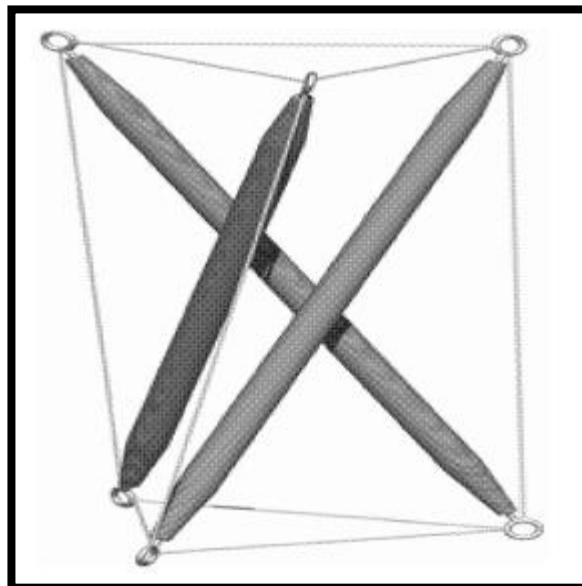


Figure 1.3: An example of prism tensegrity (Bansod et al., 2014)

The diamond tensegrity is characterised by the fact that each triangle of tendons is connected to the adjacent one with a strut and two interconnecting tendons. Figure 1.4 shows an example of diamond tensegrity.

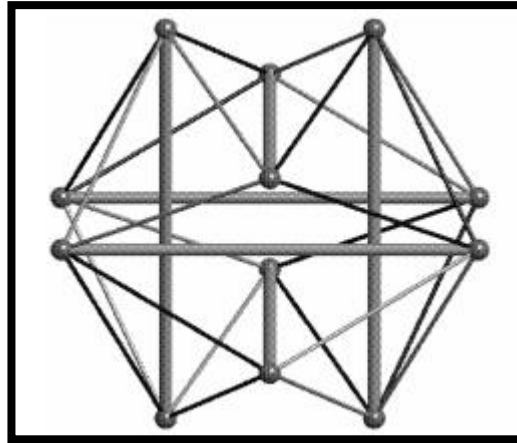


Figure 1.4: An example of diamond tensegrity (Bansod et al., 2014)

The zig-zag tensegrity is the counterpart of diamond tensegrity. The major difference between zig-zag tensegrity and diamond tensegrity is that zig-zag tensegrity has four tendon triangles where its struts are connection in a Z configuration whereas diamond tensegrity has eight tendons triangles. Figure 1.5 shows an example of zig-zag tensegrity.

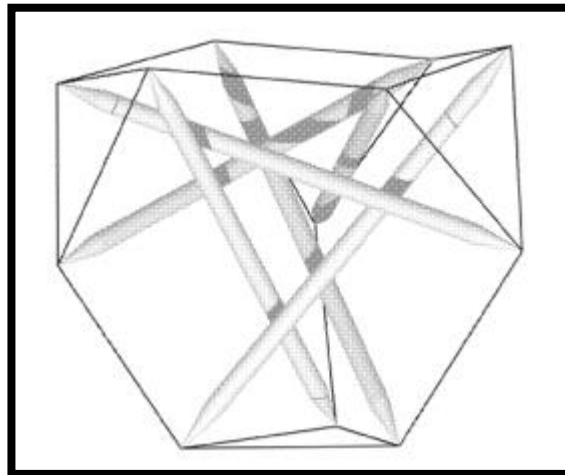


Figure 1.5: An example of zig-zag tensegrity (Bansod et al., 2014)

The prism tensegrity is the focus of the study. This is because the dominant advantage of prism tensegrity system is its ability to combine easily (Tibert and Pellegrino, 2003). The combination of two or more single-layer prism tensegrity forms multi-layer prism tensegrity. Figure 1.6 shows the formation of multi-layer prism tensegrity from two single-layer prism tensegrity.

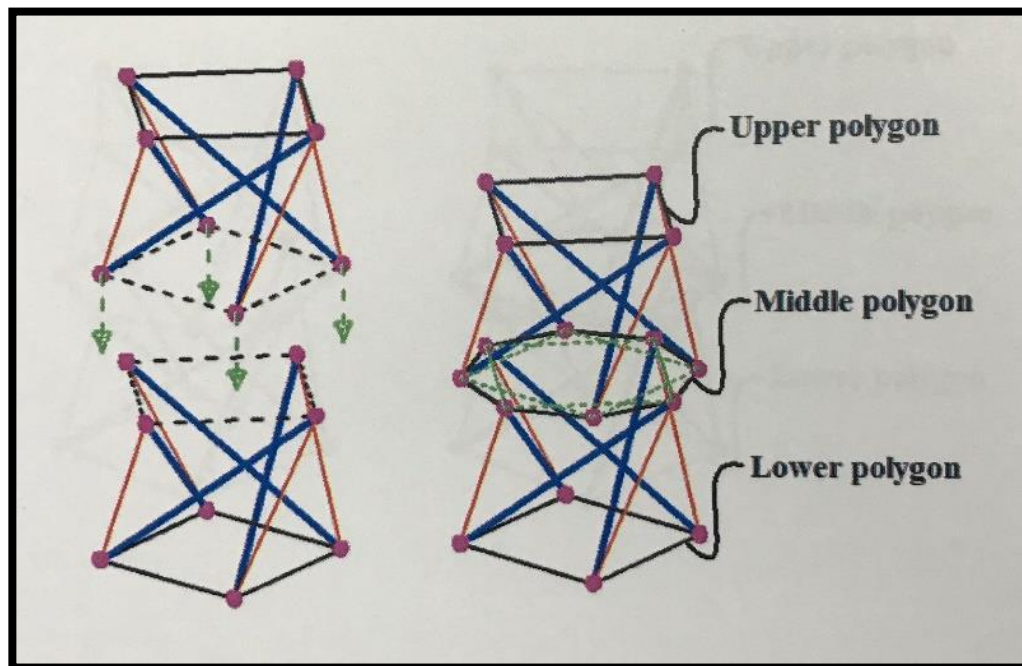


Figure 1.6: Formation of multi-layer prism tensegrity from two single-layer prism tensegrity (Mohammad, 2016)

The second advantage of prism tensegrity is its ability to form various configurations such as dome, spheroid, column, arch, and tower by using multi-layer prism tensegrity (Mohammad, 2016). This characteristic of the multi-layer prism tensegrity allows the reduction in individual size and total mass of the compression elements which makes it a lightweight structure compared to ordinary structures (Buckminster, 1962). Figure 1.7 shows some examples of multi-layer prism tensegrity.

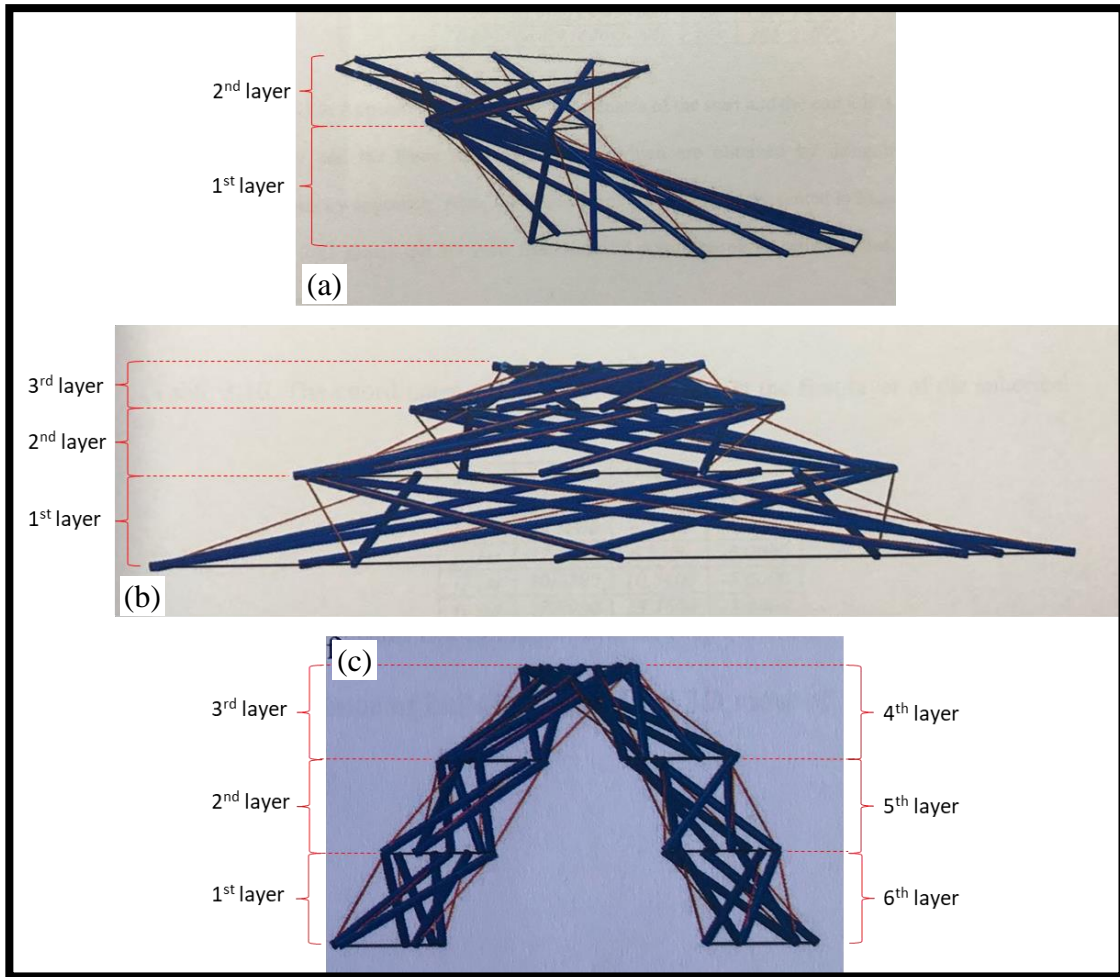


Figure 1.7: Example of multi-layer prism tensegrity (a) double layer tensegrity structure, (b) triple layer tensegrity structure, (c) six-layer tensegrity structure forming into an arch structure (Mohammad, 2016)

The various configurations of prism tensegrity allowed its shape to be either regular or irregular (Ong, 2017). Regular prism tensegrity consists of symmetrical top ring and bottom ring. On the other hand, irregular prism tensegrity consists of unsymmetrical top ring and bottom ring, thus giving designers more freedom and creativity when designing tensegrity structures. Figure 1.8 shows some examples of irregular prism tensegrity.

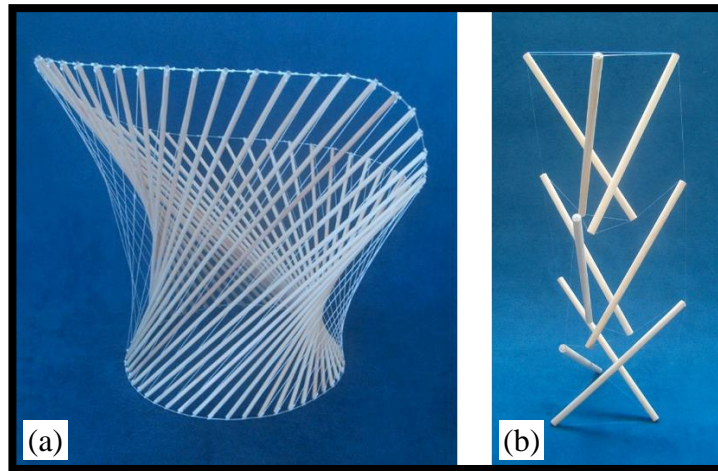


Figure 1.8: Examples of irregular prism tensegrity (a) single-layer tensegrity, (b) multi-layer tensegrity (www.tensegriteit.nl)

White Rhino is the world's first tensegrity structure built at Chiba in Japan in June, 2001. This tensegrity structure uses the configuration of irregular prism tensegrity in its design. Two irregular prism tensegrities were constructed to support the membrane roofs (Kawaguchi and Shunji, 2009). Figure 1.9 shows the interior view of White Rhino.



Figure 1.9: Interior view of White Rhino (Kawaguchi and Shunji, 2009)

1.2 Problem Statement

Many research studies on form-finding method for tensegrity has been carried out. Some research studies introduce new methods of form-finding for tensegrity while other research studies improve the previous methods of form-finding for tensegrity. However, in comparison with research studies on form-finding, studies or literature on construction sequence of full scale tensegrity structures is relatively lacking.

The construction of tensegrity structures is challenging due to its high sensitivity where its shape is unstable during construction. The construction of tensegrity poses challenges as the structure will not be stable and rigid until the desired pre-stressing forces in the correct ratio are introduced in all its members. The construction is closely related to the sequence of connecting members (cables and compression struts) and application of pre-stressing forces. In comparison with single-layer prism tensegrity, the construction of multi-layer prism tensegrity will be even more difficult. This is due to the reason of the sharing of a common ring between two consecutive layers and the inter-relation among members in different layers. Any difficulty faced in the introduction of pre-stressing forces or erection sequence in the lower layer is expected to cause problem to the higher layers. Results of study on construction sequence of single layer prism tensegrity should be further extended to the construction of multi-layer prism tensegrity. Specifically, study on application of form-finding results to the eventual construction of multi-layer prism tensegrity considering critical issues such as method of temporary holding of members and difficulties in the connection between consecutive layers need to be studied.

1.3 Objectives

The objectives of this study are:

- i. To determine method of application of pre-stressing forces based on results of form-finding analysis carried out on multi-layer prism tensegrity.
- ii. To propose a practical sequence of construction of multi-layer prism tensegrity.

1.4 Layout of thesis

Chapter One describes the background, problem statement and objectives of this study.

Chapter Two presents the review of various form-finding methods of tensegrity by previous researchers. Existing tensegrity structures are studied. The construction sequence of irregular single layer prism tensegrity structure is reviewed.

Chapter Three describes the procedure of form-finding of tensegrity, selection and testing of materials, and determination and validation of construction sequence through physical modelling of irregular multi-layer prism tensegrity.

Chapter Four presents the results and discussions of the physical models constructed. The determination and validation of construction sequence of the physical models are discussed.

Chapter Five presents the conclusions and recommendations of the study.

CHAPTER 2

LITERATURE REVIEW

2.1 Form-finding of tensegrity structure

For a tensegrity structure to achieve self-equilibrium, the determination of geometrical configuration or known as form-finding of tensegrity structure is required. There are various methods of form-finding of tensegrity structures by many researchers. Tibert and Pellegrino (2003) conducted a classification and review of seven form-finding methods of tensegrity structures into two major categories which are kinematical methods and statical methods. There are three methods which falls under the kinematical methods which are analytical solutions, non-linear programming and dynamic relaxation. Four methods are classified under statical methods which are analytical solutions, force density method, energy method, and reduced coordinates. The first category of methods, the kinematical methods, determine the geometry of a tensegrity structure by maximising the lengths of the struts while maintaining the length of the cables as a constant. The analytical solution of kinematical methods has an advantage due to its simplicity. However, the formulation becomes infeasible when many variables are required to define the configuration. The non-linear programming has a similar disadvantage compared to analytical solution where the number of constraints equations increases with the increase of the number of elements. The non-linear programming is not suitable for larger tensegrity systems. The dynamic relaxation method has good convergence properties for systems consisting a few nodes. However, this method is ineffective when the number of nodes in the system increases which restrict the method when applying in irregular structural forms. The second category of methods, the statical methods, set up a

relationship between equilibrium configurations of a structure and the forces in its members. Both analytical solution and force density method establish linear nodal equations of equilibrium in terms of force densities and the equations are solved for the nodal coordinates. The advantage of the force density method is that it is suitable when the lengths of the elements of the structure are not specified. The energy method is based on an energy minimisation approach to produce a matrix identical to the force density method. This method has introduced super-stable tensegrity structures. The reduced coordinates method achieves the equilibrium configurations of a set of rigid bodies by solving a reduced set of equilibrium equations. The advantage of this method is that it has greater control on the shape of the structure.

Many other researchers have also introduced new methods and improved previous methods of form-finding of tensegrity structures. Li et al. (2006) studied a form-finding method based on the dynamic relaxation method with kinetic damping. An appropriate choice of related stiffnesses is used to fix the force or length of some elements. This method can achieve new tensegrity configurations which are more intricate and creative. Zhang et al. (2006) presented the adaptive force density method for form-finding of tensegrity structures. This method is based on the eigenvalue analysis and spectral decomposition of the equilibrium matrix with respect to the nodal coordinates. This method has a strong ability in searching new configurations by changing the initial set of force densities and the nodal coordinates. Koohestani et al. (2013) presented a new form-finding method using combined formulation of the equilibrium and geometrical compatibility equations, which is a counterpart of the force density method. This method is suitable for moderately large and irregular models. However, the method has a disadvantage where its solution is not guided to super-stable configurations. Ehara et al. (2010) presented a form-finding method using numerical method based on the ground

structure method by solving mixed integer programming problems sequentially. In this method, the connectivity information of cables and struts are not required in advance while achieving the desired configurations. Zhang et al. (2014) presented a form-finding method based on the structural stiffness matrix. The self-equilibrated and stable state of the structure is achieved by using stiffness matrix and potential energy of the structure to converge the structural configuration. This method is highly efficient for both regular and irregular large-scale tensegrity structures. Lu et al. (2015) used matrix iteration as a form-finding method to obtain self-stress and coordinates. This method can be applied to irregular tensegrity structures which satisfy given geometrical forms. Mohammad (2016) presented a form-finding method which is a linear approach by combining length relation condition and force equilibrium equation. The configuration of multi-layer tensegrity structures can be achieved accurately and rapidly using this method. New configurations of prism tensegrity such as branching prism tensegrity is also achieved using this method. A computational tool which can design regular and irregular prism tensegrity with immediate results is also developed.

2.2 Construction of tensegrity structure

White Rhino is the world's first tensegrity structure built at Chiba in Japan in June 2001. Figure 2.1 and Figure 1.9 show the exterior and interior view of the White Rhino respectively. The structure is made up of two single layer prism tensegrities with different heights. The height of the first prism tensegrity is about ten metres whereas the second prism tensegrity is about seven metres in height (Kawaguchi and Shunji, 2009). Each prism tensegrity is used to support an isolated post member which in turn supports

the membrane roof of the building. Figure 2.2 shows the plan and section view of the building.



Figure 2.1: Exterior view of the White Rhino (<https://www.iis.u-tokyo.ac.jp>)

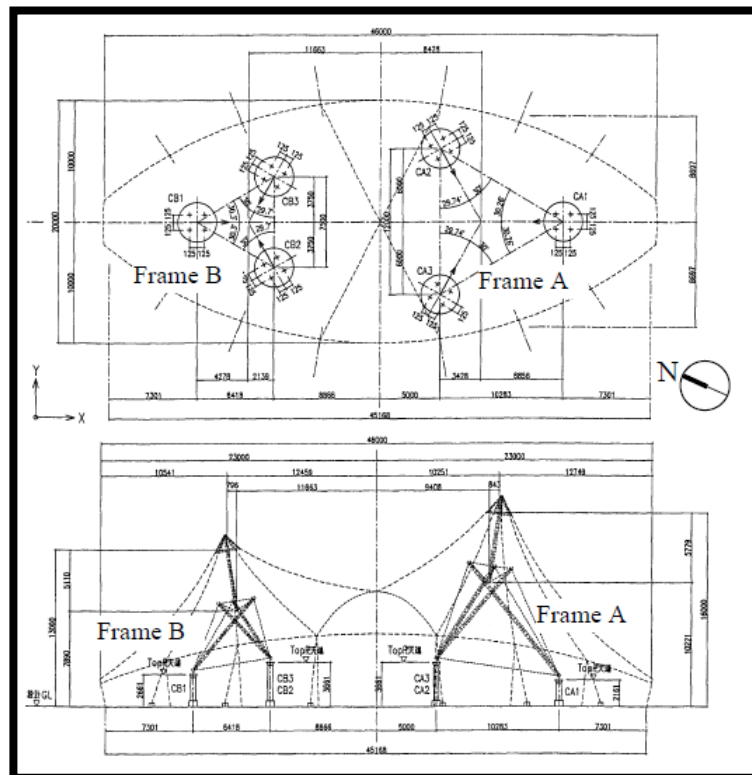


Figure 2.2: Plan and section view of the White Rhino (Kawaguchi and Shunji, 2009)

The literature on the construction details of the White Rhino is insufficient. There is one video clip showing the construction process of the White Rhino. However, there is no detailed description on the construction process itself. Figure 2.3 shows the video clippings of the construction process.



Figure 2.3: Video clippings showing the construction process of the White Rhino (<https://www.youtube.com/watch?v=IeWWPAckC5U>)

The La Plata Stadium in Argentina uses a different configuration of tensegrity compared to that of the White Rhino. The configuration of tensegrity of the La Plata Stadium shapes like a dome. The tensegrity roof network features tensioned steel cable hoops at three different levels with vertical struts (tensegritywiki). Figure 2.4 and Figure 2.5 show the interior view and the schematic roof frame of the building respectively. In

the aspect of the construction process, only images during the construction phase of the building are available without any detailed descriptions. Figure 2.6 shows the images during the construction phase of the building.

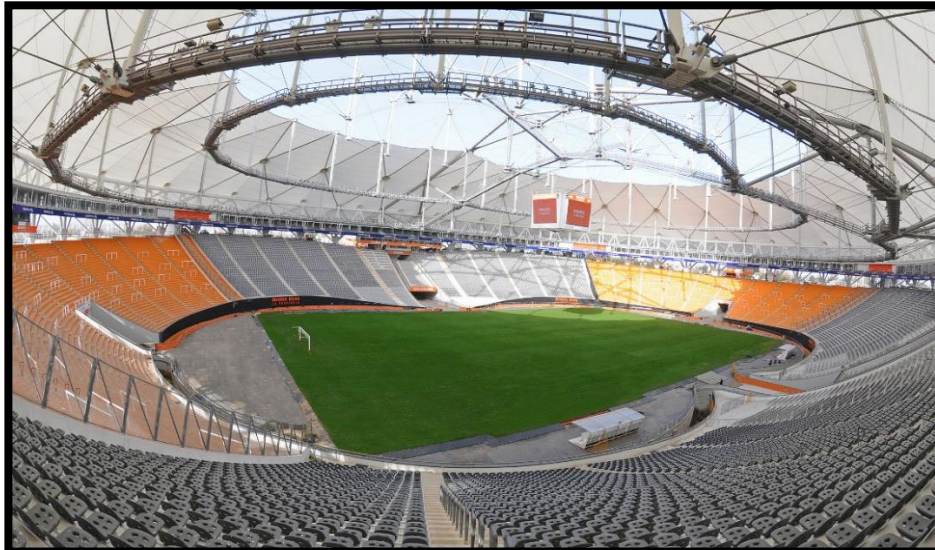


Figure 2.4: Interior view of the La Plata Stadium
(<http://www.stadiumguide.com/ciudaddeplata/>)

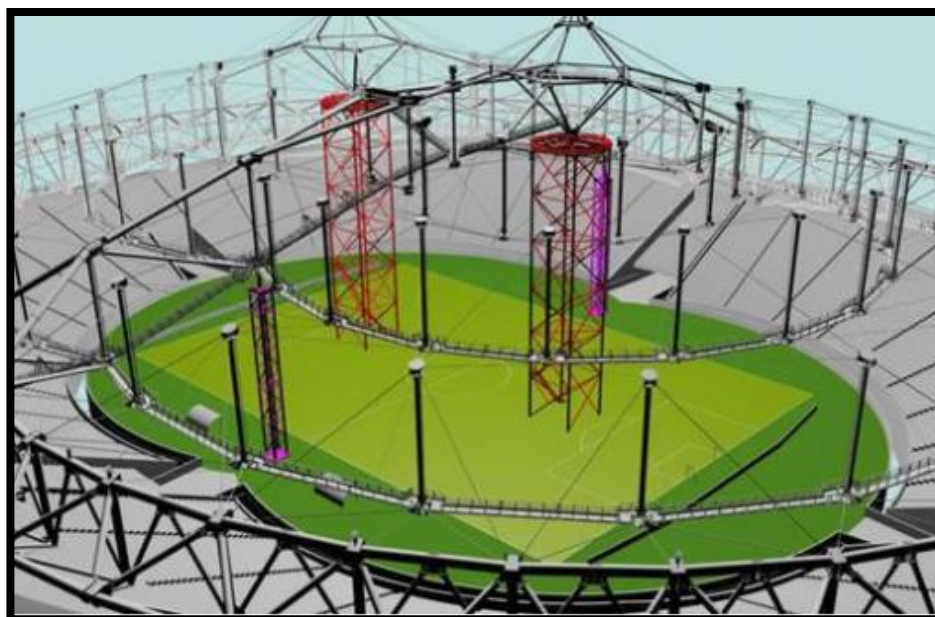


Figure 2.5: Schematic roof frame of the La Plata Stadium
(<http://tensegritywiki.com/La+Plata+Stadium>)



Figure 2.6: Images during the construction phase of the La Plata Stadium (<https://www.gettyimages.com/event/construction-of-ciudad-de-la-plata-stadium-106786978#general-view-of-the-ciudad-de-la-plata-stadium-construction-on-19-picture-id107087733>)

The Kurilpa Bridge in Brisbane, Queensland, Australia is the world's first tensegrity pedestrian and cycle bridge. The bridge was completed and opened to pedestrian in October 2009 (A pedestrian and). The tensegrity bridge consists mainly of composite steel and concrete deck structure. Other members include series of steel masts

and cables, integrated array of steel ties, flying struts and steel-framed tensegrity canopy (Oasys Software Case). Figure 2.7 shows the completed structure.



Figure 2.7: The Kurilpa Bridge in Australia completed in October 2009
(<https://www.arup.com/projects/kurilpa-bridge>)

In order to ensure that the large complex structure can be completed with the correct geometry, the components of the bridge are prefabricated to the desired dimensions. During the connections of the members, adjustment is not required to achieve the desired geometry. Various scenario planning and sophisticated analysis has been carried out by Arup to check every stage of the construction. Figure 2.8 shows the modelling and design of the bridge at different construction stages. The modelling is proved to be accurate when two spans of the bridge met precisely in the middle (Oasys Software Case).

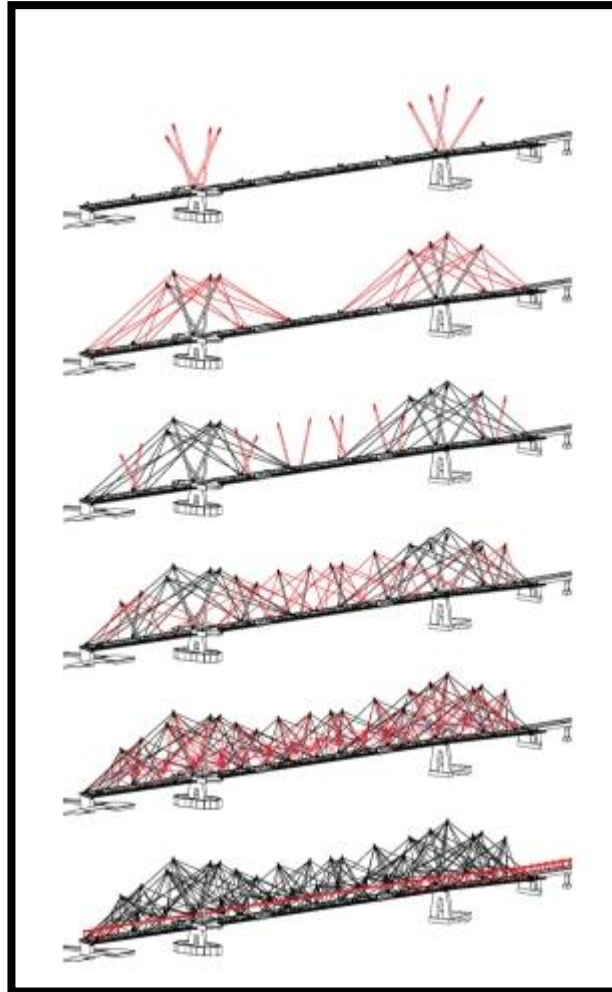


Figure 2.8: The modelling and design of the bridge at different construction stages (<http://www.oasys-software.com/solutions/case-studies.html?id=64/>)

A study on the construction sequence of irregular single-layer prism tensegrity has been carried out by Ong (2017). The linear approach method of form-finding using force ratio calculation developed by Mohammad (2016) was used in the study. Three laboratory scale models (50mm, 260mm, and 260mm in height) have been built and an actual practical scale model (1.8m in height) has been erected. Figure 2.9 and Figure 2.10 shows the laboratory scale models and the actual practical scale model respectively. Two different shapes were used in the study which are triangular prism and quadrilateral prism. These two shapes were chosen because they are the basic shapes of prism tensegrity.

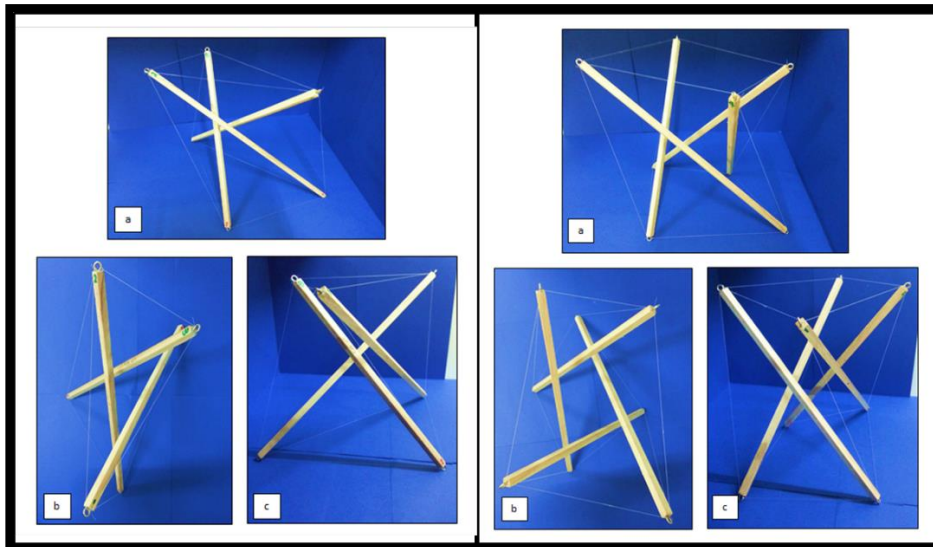


Figure 2.9: Laboratory scale models in triangular prism (left) and quadrilateral prism (right) with a height of 260mm (Ong, 2017)



Figure 2.10: Actual practical scale model with a height of 1.8m (Ong, 2017)

Ong (2017) has come out with a validated construction sequence of the tensegrity models which are as follows: (i) struts are placed at the supports, (ii) cables of the bottom ring

are connected, (iii) cables of the top ring are connected, (iv) cables of diagonal ring are connected, (v) cable with the highest tension is connected. The construction sequence is validated by comparing the coordinates of the model with the coordinates from the form-finding analysis.

2.3 Summary

Many research studies on form-finding method for tensegrity has been carried out. New methods of form-finding have been introduced by some researchers while others improved previous methods of form-finding. Some full-scale tensegrity structures in the world have been constructed. However, there is no detailed documentation on the construction sequence. In comparison with research studies on form-finding, studies or literature on construction sequence of full-scale tensegrity structures are relatively lacking. The construction sequence on single layer tensegrity has been studied by Ong (2017). As multi-layer prism tensegrity is expected to be more complicated to be built, extension of the study by Ong (2017) to the case of construction of multi-layer prism tensegrity is needed.

CHAPTER 3

METHODOLOGY

3.1 Overview

This project is a follow-up study to the work carried out by Ong (2017). The construction sequence of single-layer prism tensegrity presented by Ong (2017) is used as reference in this project. The construction sequence is further extended for multi-layer prism tensegrity. The main study and the challenge in this project is to investigate the construction sequence of tensegrity structures involving more than one layer by combining two or more single-layer tensegrity structures.

Form-finding of tensegrity structures is required to obtain the desired configuration of the tensegrity structure before construction begins. A computational tool developed by Mohammad (2016) is used to carry out form-finding analysis. The tool uses a linear approach by combining length relation condition and force equilibrium equation. The configuration of multi-layer tensegrity structure can be obtained accurately and rapidly with the aid of the computational tool. The form-finding analysis is started by carrying out data input. The data required for form-finding analysis include coordinates of first ring, azimuth angle of first and last member of second ring, coordinates of first joint of second ring or coordinates of centroid of second ring, and scale ratio of second ring, first and second conjunction polygon. The output data from the form-finding analysis include coordinates of subsequent ring, the lengths of each members (cables and struts) and the force ratios of the members of the structure.

After form-finding analysis has been carried out, physical modelling is conducted to investigate the construction sequence of tensegrity structures. Construction materials

of cables and struts are selected. A tensile test is carried out to determine the strength capacity and elongation properties of the cables and the connections. A graph of force against elongation is obtained from the tensile test. A force factor is applied in the calculation of the pre-stress required for each member. A force factor is a value multiplied to the force ratio to obtain the actual pre-stressing force to be introduced to the cables so that the actual pre-stressing force will not exceed the maximum load capacity of the cable.

The physical modelling is carried out at laboratory scale before proceeding to the actual practical scale. The purpose of laboratory scale modelling is to obtain a practical construction sequence before applying the sequence to actual practical scale. This is because laboratory scale modelling is lightweight and easier to handle compared to the modelling of actual practical scale. Lastly, the construction sequence obtained from laboratory scale modelling is applied to the modelling of actual practical scale for verification and validation. Figure 3.1 shows the summary of the methodology of the research.

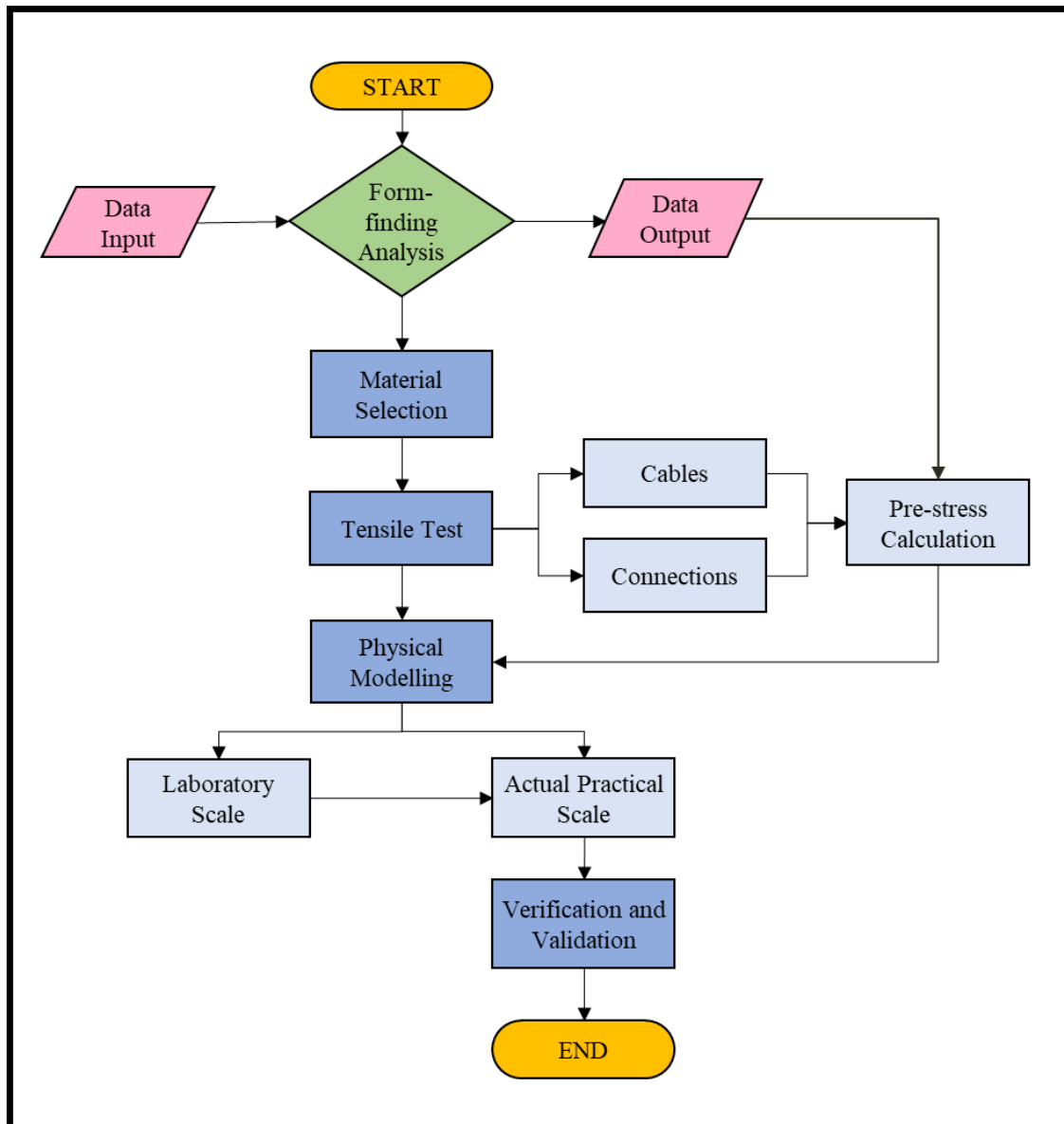


Figure 3.1: The flow chart of research methodology

3.2 Form-finding of tensegrity

Form-finding of tensegrity is required to obtain the configuration and self-equilibrium of the structure. Form-finding analysis is carried out by using a computational tool developed by Mohammad (2016). The components of a prism tensegrity must be identified for the analysis to work. A prism tensegrity consists of two polygons parallel to each other in the same plane, which is the xy-plane. The height of

the tensegrity is measured along the z-axis which is perpendicular to the xy-plane. The lower polygon is called the first ring whereas the upper polygon is called the second ring. The number of vertices for each polygon is denoted by n . A particular joint in the system is denoted by i where $i \in (1 \text{ to } n)$. The joints of the first and second ring are denoted by j_i and j'_i respectively. The members of the first and second ring are denoted by l_i and d_i respectively. The internal angles at the first joint of the first and second ring are denoted by α_i and β_i respectively. The azimuth angle is the angle at the first joint between the first member of each ring and the x-axis and is denoted by α'_i and β'_i for first ring and second ring respectively. The diagonal tension members and compression members are denoted by t_i and c_i respectively. The polar angle is the angle between the diagonal members and the xy-plane and is denoted by δ_i and γ_i for compression members and tension members respectively. The azimuth angles of compression members and tension members are denoted by φ_i and ν_i respectively. Figure 3.2 shows the six joints of the first and second polygon with their connected members.